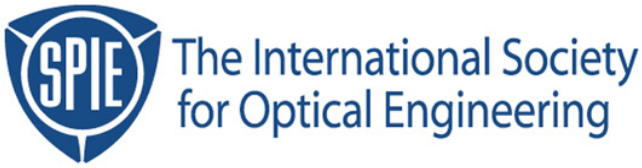

This paper was published in the proceedings of the
21st Annual BACUS Symposium on Photomask Technology
SPIE Vol. 4562, pp. 486-495.

Characterization of Quartz Etched PSM Masks for KrF Lithography at the 100 nm node

P. Rhyins[1], M. Fritze[2], D. Chan[3], C Carney[4], B.A Blachowicz[4], M. Vieira[4,] C. Mack[5] of 1) Photronics, Inc., Allen, TX 75013, 2) MIT Lincoln Laboratory, Lexington, MA 02420, 3) Photronics, Inc., Austin, TX 78728 4) ARCH Chemicals, INC 5) Finle Technologies, KLA Tencor Corp

ABSTRACT:

The application of strong phase shift masks (PSM's) such as AAPSM and Chromeless using KrF 248-nm lithography is increasingly in demand for production of advanced devices at the 130 nm node and below [1,2,3,4]. Implementation of dual exposure PSM technology [5,6,7] is becoming widely accepted as a method to achieve sub-wavelength gate and contact layer resolution for microprocessors, DRAM and thin film heads. This requires a stable and repeatable phase-shift mask process that will perform for the wafer lithographer and is manufacturable using today's leading edge photomask fabrication methods.

The focus of this study is the characterization of the photomask quartz etch process. The effect of the photomask's phase depth control and the quartz etch CD control will be examined. A comprehensive mask metrology study will be supplemented by lithography process latitude data, both simulation and experimentally based. The effect of fabricating the photomask quartz trenches using either resist or chrome defined etch masks will also be studied as well as the impact on lithography process latitude. A key goal of this study is the determination of a realistic specification for the quartz etch process required for leading-edge phase-shift photomasks.

1. INTRODUCTION

Strong phase-shift masks, such as chromeless or alternating-aperture, are typically fabricated by a subtractive quartz etch process. The step heights required are determined by the condition for destructive interference of the incident illumination light. This is given by:

$$Z = \lambda/2(n-1)$$

Where lambda is the illumination wavelength and n is the index of refraction of the mask material. For the case of 248-nm illumination and a quartz mask, we obtain $Z = 248/2(1.509 – 1) = 244$ nm.

This study will look at the characteristics of the photomask quartz etch process across a +/- 30-degree phase variation. The PSM will be fabricated with the theoretical target depth for KrF applications given by the above formula. Lithography process latitude, both simulated and experimental, will be presented through focus, across a 30- degree phase range. Lithographic variables studied include both CD control and image placement shift. A through-phase map of lithographic performance (CD control and image shift), along with reticle phase and trench depth metrology, is presented from which optimum target and tolerances of the quartz etch are determined. These results yield phase and focus latitude permissible for state-of-the-art lithographic performance.

2. EXPERIMENT

A multi-phase mask was fabricated using manufacturing methods for Chromeless and Alternating PSM's for active device layers. Test patterns comprised of isolated and dense lines were created using two methods, one with chrome and one with resist as the quartz etch mask. Twelve identical test cells were provided with quartz trench depths ranging from 155 to 210 degrees in steps of 5 degrees.

Common mask metrology tools were used to measure the quartz depth and phase. These tools, a KLA Tencor P12EX profilometer and Lasertech MPM 248 are used in production to disposition PSM reticles. Data from these tools will be compared to the Surface Interface SNP 9000 Nano Profiler. Wafer exposures were performed on a Canon EX-6, 248-nm stepper with Arch Chemical GKRS 5106 resist. An NA of 0.65 and sigma of 0.3 was used. Through phase and through focus resist CD was measured on a KLA Tencor 8100 CD SEM.

Simulation was performed using Finle Technologies ProLith software to predict CD variation and image shift through phase and focus. A full electromagnetic mask simulation model was used provided by Finle Promax software.

3. PHOTOMASK FABRICATION

The photomask employed for this experiment is a 5X reticle fabricated on a 6-inch standard chrome and quartz blank. A layout of 12 pattern cells (see figure 1) were placed in a 4 x 3 array across a 110 mm x 125-mm field size. Mask patterns include isolated and dense line from 0.25 um through 2.0 um and a depth and phase monitor pattern that has trench widths from 50 um down to 0.25 um.

Figure 1

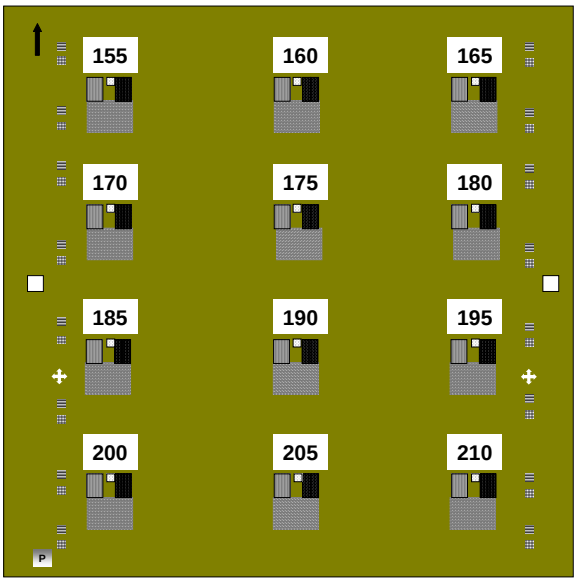

Variable Phase Mask Layout

The chrome binary level patterning was done on an ETEC Alta 3500 laser writing tool with IP 3500 resist and processed using a Unaxis VLR 700 ICP dry chrome etch system. A second write defining the quartz-etched areas was done after re-coating the binary chrome mask with OCG 895I resist And an aligned write on an Alta 3000 laser tool. A quartz etch was then done on a Unaxis SLR 700 RIE plasma etch system. Variable phase on the reticle was created by first etching the mask to a nominal depth of 155 degrees, masking a pattern cell, and adding an additional 5 degrees to each cell. Using this method, the etch depth varied by 65 angstroms per cell, where the total phase range across the plate was 60 degrees in 5 degree increments. Portions of the reticle that were designed to be chromeless lines as defined by chrome, were made by a third coat, aligned write and process step. The chrome was then removed locally by a wet chrome etchant.

4. PHOTOMASK METROLOGY RESULTS

Historically, the PSM quartz trench depth has been characterized using either a stylus tip profilometer or direct phase measurements using a laser interferometer. These two methods have often given results that could not be directly compared to the theoretical phase values and wafer print data. There has been indication that an offset exists between the measured PSM data and wafer print data. In this study, the intent is to establish the metrology limitations and scope of error associated with using production equipment to fabricate PSM's. Measurements made by the profilometer and the laser interferometer show a good agreement throughout the range of phase in the experiment. (See figure 2). Figure 3 shows the difference between these two tools to be <2 degrees when both large and small feature sizes are compared. The stylus profilometer is capable of measuring quartz etched trenches down to feature sizes of

approximately 2 um and the laser interferometer is capable of measuring down to 2 um based on the minimum shear that is used. For this experiment, the interferometer shear was set to 10 um due to repeatability issues and compatibility with the current production processes, and limited the MPM 248 to measuring trench sizes of greater than 10 um.

Figure 2

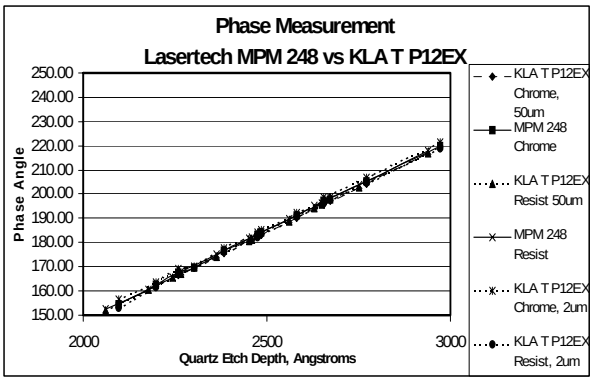

Figure 3

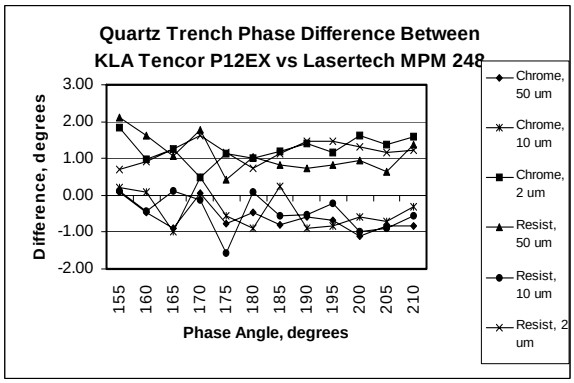

KLA Tencor and Lasertech MPM 248 data

4.1 Feature Size Dependency

The P-12EX data shows a feature size dependency of the quartz depth between a 50 um trench and a 2 um trench, where the smaller trench measures 25A deeper or 2 degrees greater phase. This is true for both the chrome-defined trench and resist defined trench, although the chrome-defined trench has a greater depth than the resist-defined trench of 25A or 2 degrees. For smaller feature sizes down to 0.5 um, the Surface Interfaces SNP 9000 Nano Profiler is used. There is good agreement between the SNP and both the profilometer and laser tool to within 0.5 degrees (see figure 4). The feature size dependency as seen with the profilometer, is supported by the SNP and shows a difference of a 2.7 um wide trench versus a 0.5 um trench of about 8.1 degrees (see figure 6).

For the 1.2 um PSM chromeless feature imaged in the wafer print results for dense lines, the offset for the chrome defined feature is +5.3 degrees compared to the laser tool. This would indicate that a PSM fabricated to the theoretical depth of 2440 angstroms would actually perform as a PSM with a phase of 185.3 degrees. If the resist defined feature is considered, then the offset is +3.1 degrees. Unless the PSM is measured at the feature size that is desired to be imaged on the wafer, the PSM target depth would be 174.7 degrees for the chrome-defined lines and 176.9 degrees for the resist defined lines.

Figure 4

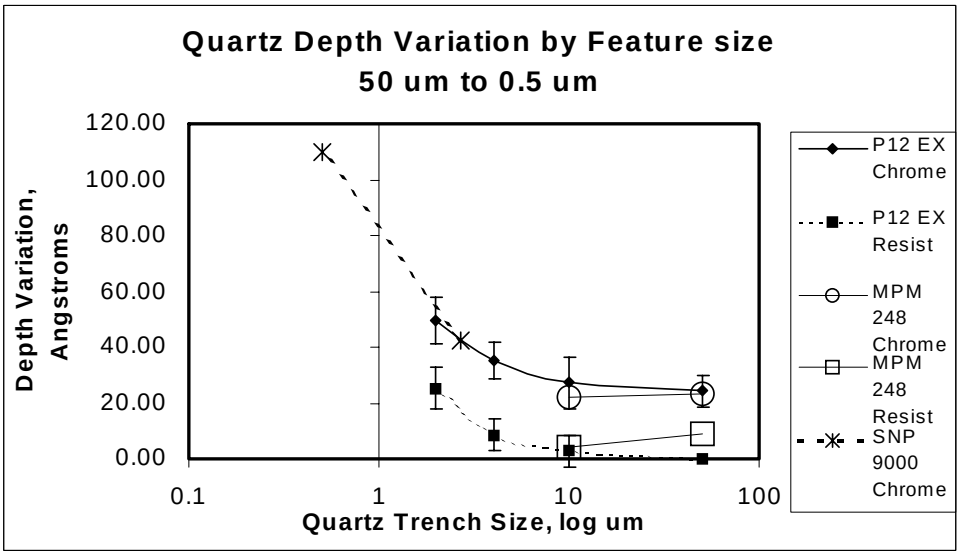

4.2 Sidewall Angle

The sidewall angle of the quartz trench, as measured by the SNP 9000, is similar for the larger 2.7 um trench and the smaller 0.5 um trench, being 81.0 degrees and 80.3 degrees respectively (see figure 5). This measurement was taken on the chrome-defined trench only, and the resist defined trench value is not known for this experiment. An explanation for the lower phase value that we see on the resist-defined trench could be that there is a shallower quartz sidewall angle. Further study is required to determine the cause.

Figure 5

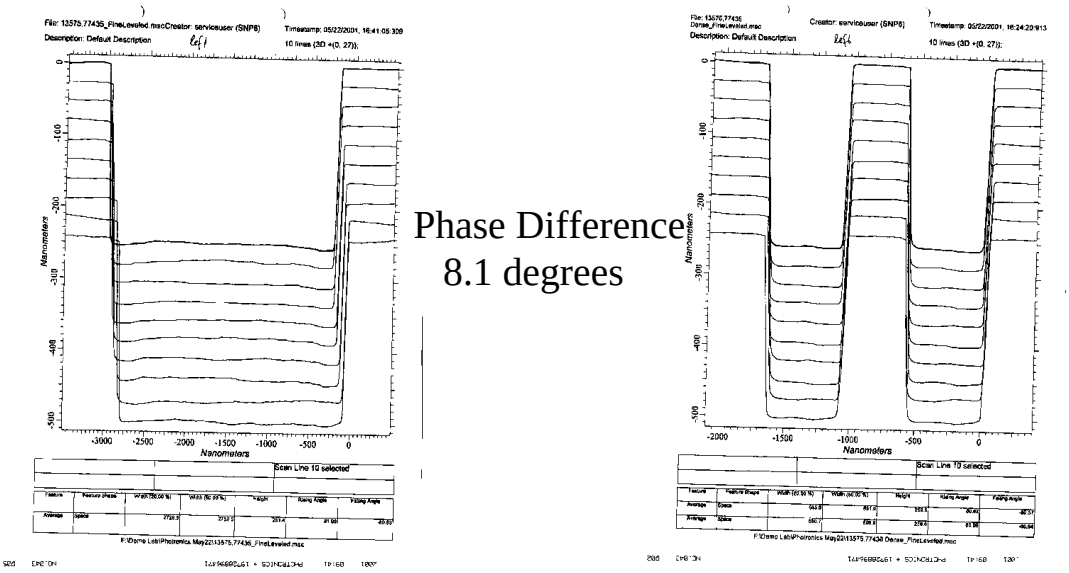

Average CD = 2.728um
Average Depth = 251nm
Range (3s) = 7.1nm
Slope=81.0 degree

Average CD = 0.614um
Average Depth = 262nm
Range (3s) = 6.4nm
Slope=80.3 degree

5. WAFER LITHOGRAPHY RESULTS

In previous studies the phase tolerance of the quartz etched PSM was gauged by the increased DOF and CD range across the field when compared to a simple binary chrome mask, [6]. Other studies show that the projected aerial image of the quartz mask feature experiences a shift in position of the feature as the reticle phase deviates from the optimum phase [8,11]. The performance specifications for PSM's have been previously thought to be limited to a narrow phase range due to image shift and DOF latitude. The ITRS roadmap [9] for the 100 nm node reports this to be +/- 2 degrees from the 180 degree optimum phase, with a 10 nm 3 sigma deviation from nominal CD to be the criteria for acceptable wafer print control.

5.1 Focus Lattitude vs. Phase

SEM CD analysis of the wafer print shows that for a DOF of 0.4 um both the isolated and dense lines formed by chromeless mask features, have a phase tolerance of +/- 15 degrees created by either chrome pattern transfer from the ALTA 3500 in the first exposure or resist pattern transfer in the second exposure on the ALTA 3000 mask write tool. The DOF of the chrome defined isolated lines is greater than that of the second write, resist defined isolated lines, (seen in figure 5-8) and SEM photos (figures 5a-8a), whereas the

dense lines exhibit the same DOF for either resist or chrome. The isolated line DOF difference may indicate a difference in the sidewall angle of the mask's quartz etched edge, where the resist formed edge has a lower contrast than that of the chrome formed edge.

Figures 5 through 8

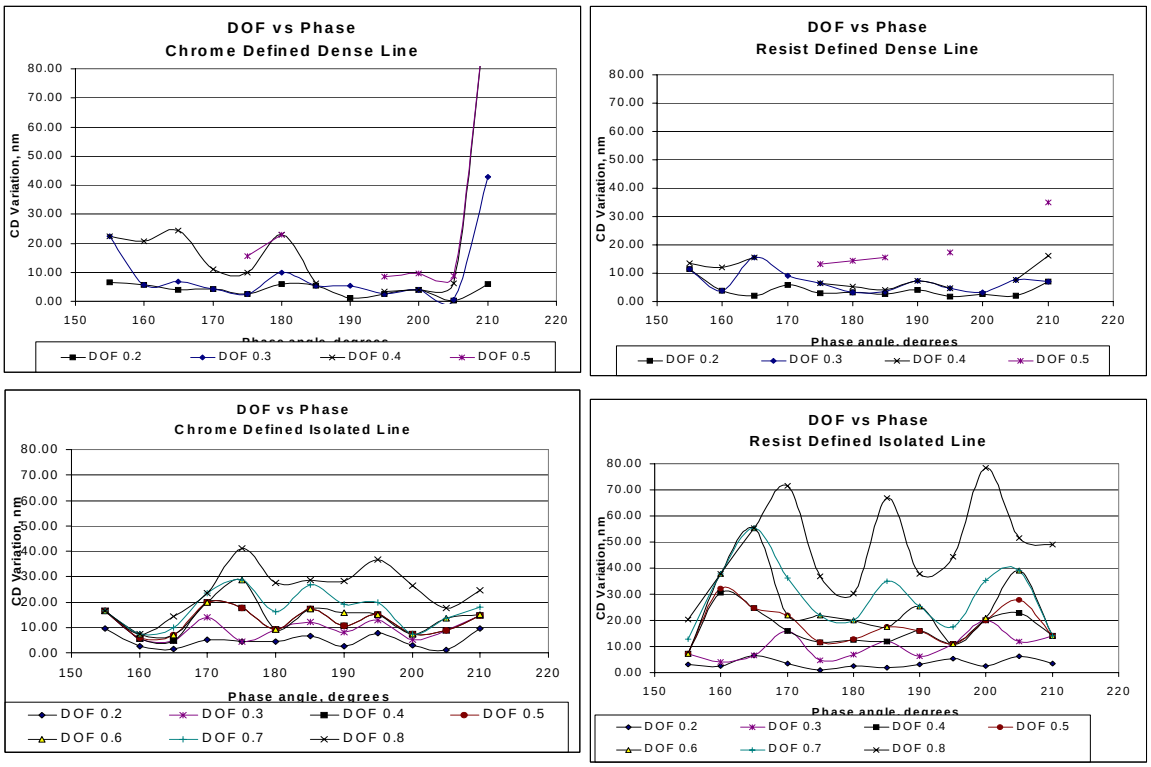

5.2 SEM Pictures of 120 nm Dense lines

Figures 5a-8a

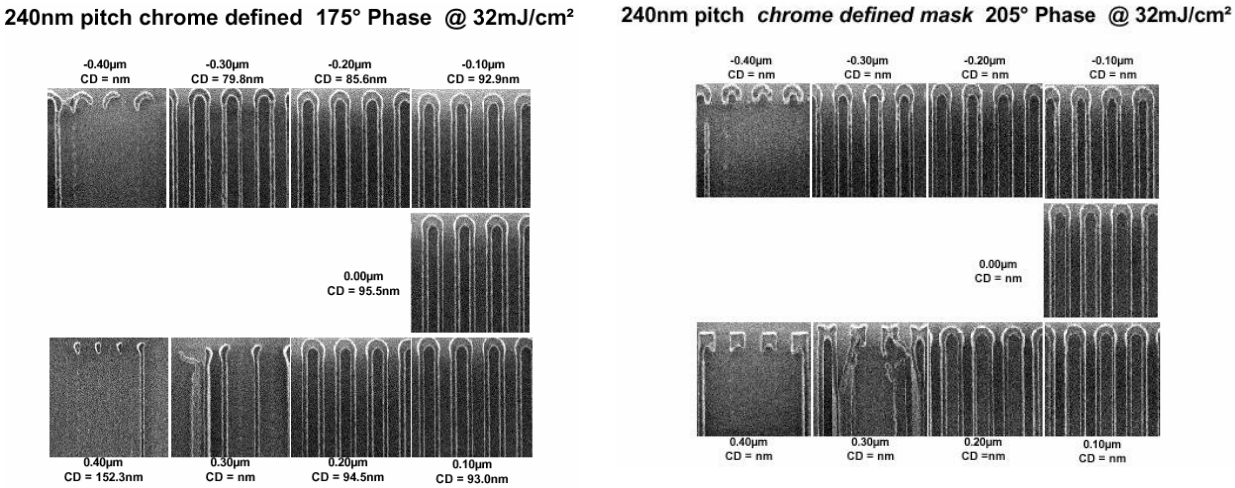

Dense Lines Defined by Chrome

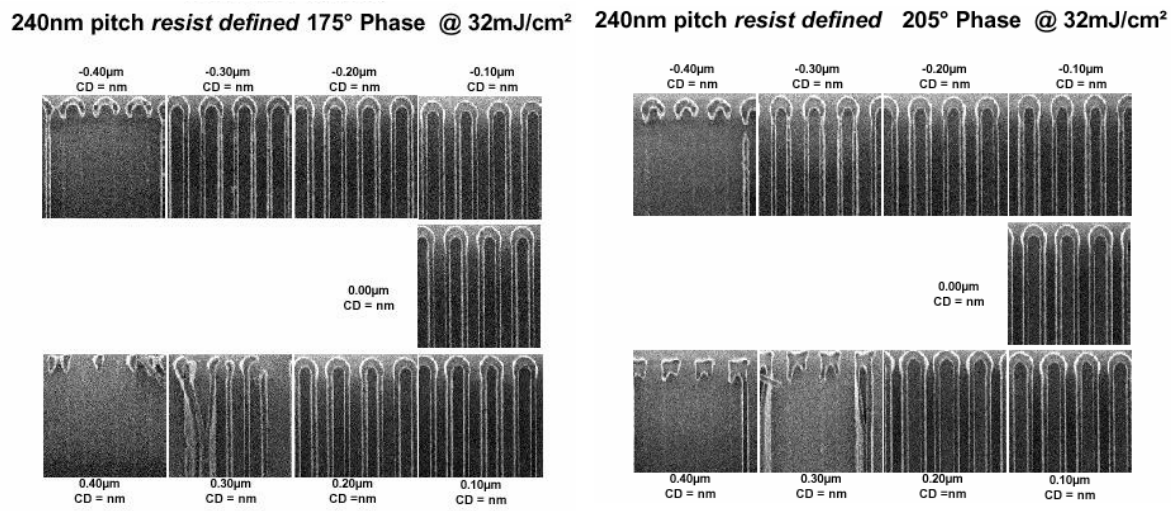

Dense Lines Defined by Resist

5.3 Image Shift vs. Phase

The SEM measurements of the chrome defined pitch, when plotted as mean pitch variation through focus, indicates that the pitch width changes with phase. The width of the pitch through focus is at the smallest variation when the phase is optimized (see figure 9). This variation can be considered to be the image shift as phase deviates from optimum phase, demonstrating the right to left CD difference of the printed chromeless lines [11, 12]. This effect can clearly be seen in the chrome defined lines but less so with the resist defined lines (see figures 10 & 11). Although the absolute pitch values are not divergent as seen with the chrome lines, the pitch variation through focus is a minimum when optimum phase is achieved. This result of the pitch variation in the resist defined mask lines can possibly be explained by the image quality, CD range, and sidewall angle of the quartz trench on the mask, behaving similarly to the reduced DOF seen in the resist defined isolated line.
Image shift can be seen to be best for dense lines from 170 degrees to 185 degrees, where the range of pitch through focus is 10 nm or less for a half pitch line pair. This behavior is the same for resist defined and chrome defined lines and spaces.

Figure 9

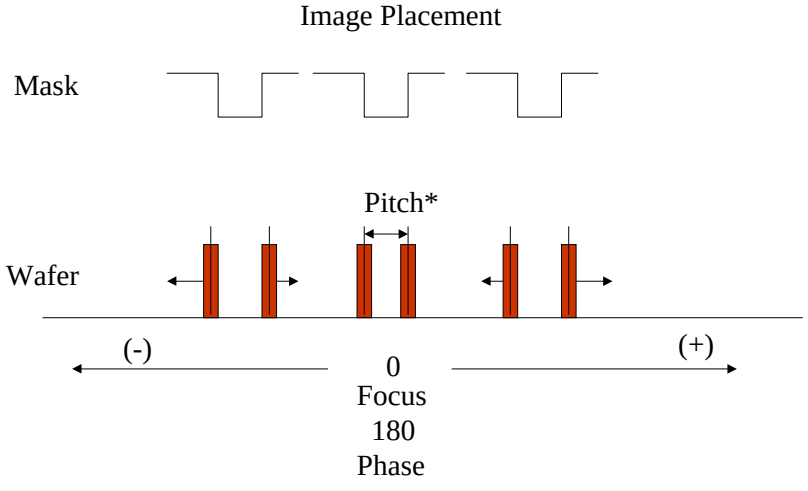

*Pitch is minimum at best phase and best focus

Figure 10 **Figure 11**

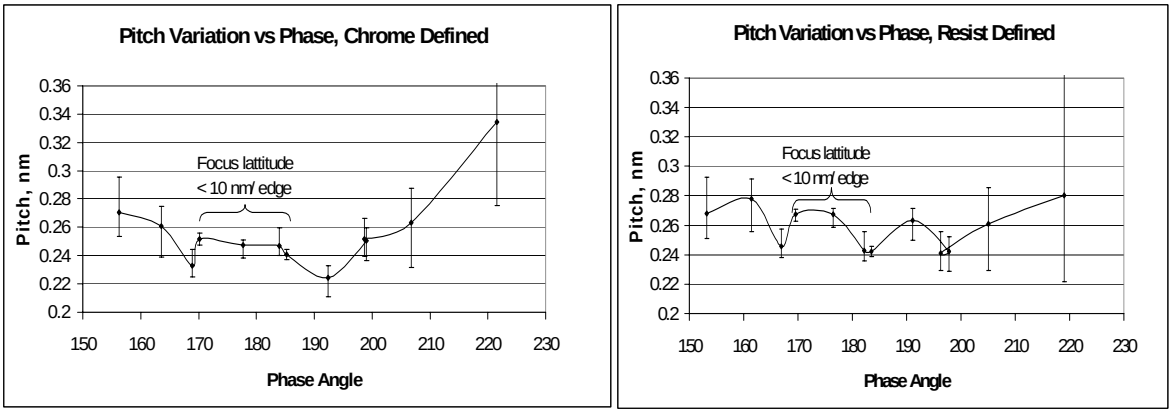

*Error bar represents pitch variation through focus

5.4 Lithographic Tool Optimization

Previous studies find that PSM focus latitude and Image shift are dependant on the lithographic tool characteristics as reported by Schenker et al [8] and that CD performance is enhanced by using a PSM. The PSM will reduce the effect of most lens aberrations thus providing superior CD control [6]. However, the DOF for a PSM has been reported to be reduced by lens coma effects, as NA is increased [11], limiting the phase tolerance to maintain a useful DOF.

5.5 Best Focus

Our wafer results show a best focus dependence on peak phase of the PSM (see figure 12) for dense lines. The sinusoidal curve seen show that the dense line and pitch have a best focus shift of 0.2 to 0.3 um for every 7 to 8 degrees of phase change. This curve demonstrates that the exposure tool focus needs to be matched to the peak phase of the reticle when determining best focus. When this is achieved, the DOF of the PSM is seen to be flat from 160 to 205 degrees for dense lines. The useful DOF of 0.4 um at a high NA of 0.65 is seen across a wide phase range for the chrome defined isolated line.

Figure 12

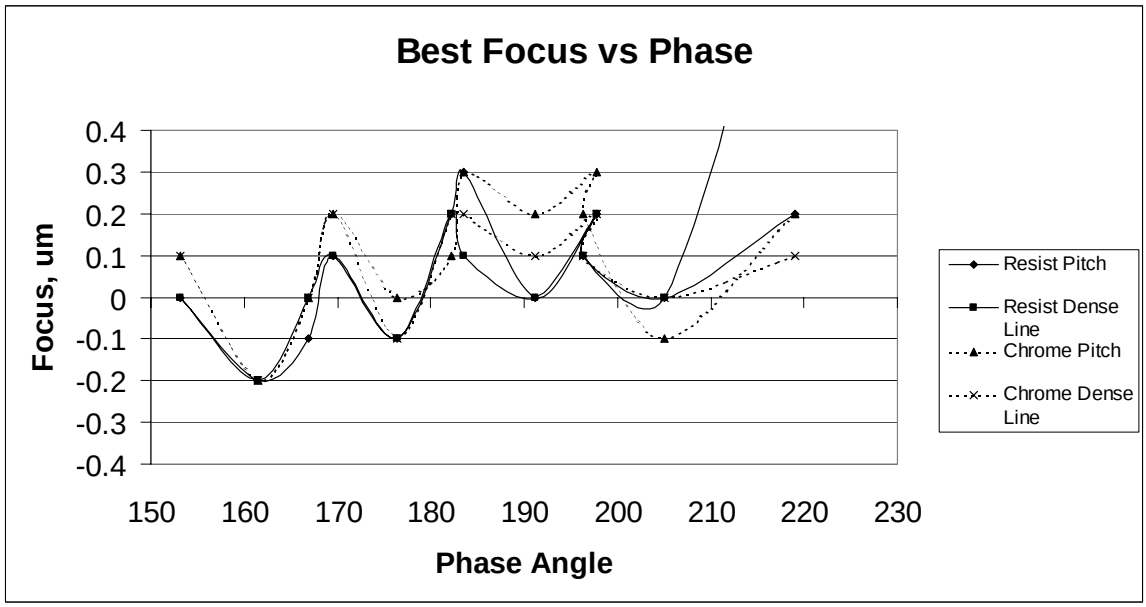

6. LITHOGRAPHY SIMULATION

Phase tolerance for best DOF and CD control has been a contested subject in previous simulation work [8], and the sensitivity to phase error was quite large for a chromeless isolated line, showing a CD error of 10 nm from 120 degrees through 190 degrees [10]. Many theoreticians have thought that the mask topography effects were not fully considered in these studies [10,11]. We present simulations of the exposure conditions, which address this issue. A full electromagnetic model for CD and image shift is employed (see figure 13 & 14) which includes 3D mask topography effects in the lithographic simulation. The electromagnetic mask simulation was performed using Promax and the simulated mask files were then read into Prolith for process latitude simulation. For these simulations, the dense feature pitch was 250 nm and the stepper NA=0.6 corresponding to a k1 factor of 0.3. This is close to the k1 factor used in our experiments , obtained from dense features of 240 nm pitch and NA=0.65. From Figs 13 & 14, lithography process latitudes as a function of phase and focus can be estimated.

Using a standard Prolith simulation (see figure 15 & 16), not taking into account mask topography effects, focus latitude through phase indicated a phase tolerance of +/- 20 degrees for a DOF of 0.4 um with the exposure conditions used in our experiment. When the full electromagnetic model (Promax) was used, this range was reduced to +/- 15 degrees. The image shift, through-phase simulations, performed using ProMax, show that for a DOF of 0.4 um, the acceptable phase range is from 174 through 188 degrees, slightly offset from a nominal phase of 180 degrees. The image offset is present for all phase values from 162 through 207 degrees at best focus, and is 8 to 9 nm. Considering this offset, the experimental data would suggest an even greater phase tolerance with respect to image shift.

Figure 13

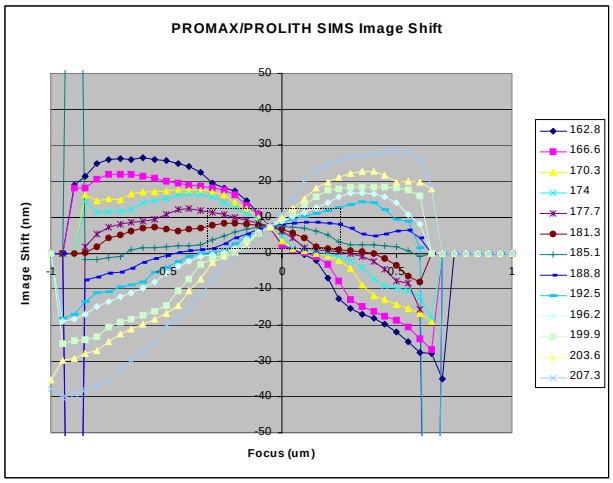

Figure 14

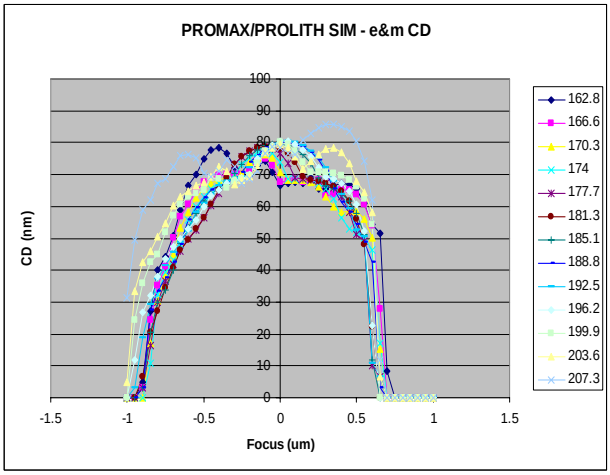

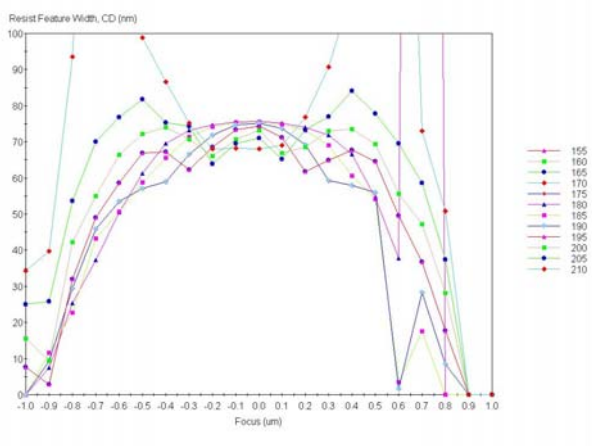

Figure 15
Prolith Calibrated Resist Model, Dense Lines

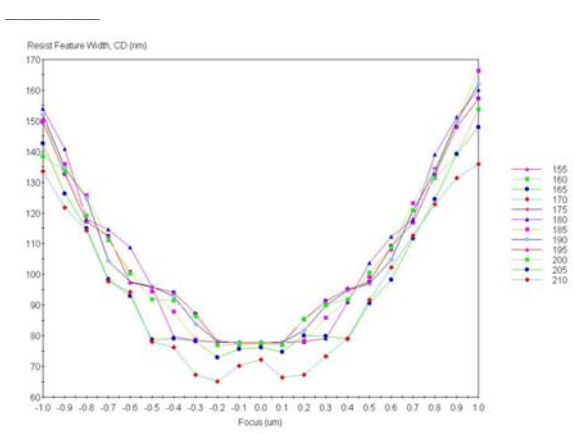

Figure 16
Prolith Calibrated Resist Model, Isolated Lines

7. CONCLUSIONS

Strong phase shift masks, such as Chromeless and Alternating Aperture, have become increasingly popular in the microlithography community in order to extend the resolution of KrF exposure tools to the subwavelength-regime of 100 nm and below. This has placed demands on the mask-maker for well-understood quartz etch process. In this work, the Photronics quartz etch process has been evaluated and characterized.

A phase-shift etch process test mask was employed, characterized by a number of common mask metrology tools. Results from this variety of metrology tools show that there is good phase depth agreement between the Lasertech, KLA Tencor and SNP 9000 of less than 2 degrees. Data from the stylus based tools show a feature size dependency of the phase and an offset of 4-6 degrees from the phase as measured on larger feature sizes when compared to the mask features that would be printed on the wafer. This data is supported by the experimental wafer prints' optimum phase for minimum image shift, determined to be 177 degrees. Additionally, resist defined quartz trenches exhibit a lower phase than the chrome defined trenches of about 2 degrees. Implementation of metrology to measure the as printed features will be necessary to meet the 100 NM KrF node.

The wafer print data shows that a DOF of 0.4 um is maintained through a wide range of phase, from 165 to 195 degrees. Image position offset is shown to be < 10 nm from 170 through 185 degrees. Dense line data shows a unique focus position dependency compared to the mask's phase. These results may be due to the stepper lens aberrations (particularly coma) and an interaction with the PSM, and will need to be characterized by the PSM user to optimize their stepper and process.

A model-based study of wafer CD control and process latitude as a function of a wide range of phase depth was presented. These simulation results were compared with experimental wafer data and shown to be consistent with the experimental data when the reticle metrology offset was considered.

Comparison of the experimental wafer results with the mask metrology data provided an understanding of the phase etch depth tolerance acceptable for typical microlithography applications. This study has found an acceptable phase tolerance of +/- 8 degrees based on image shift as the most sensitive lithographic effect.

FUTURE WORK

There is still much more to understand about the behavior of the quartz trench sidewall angle and it's impact on phase performance and wafer print results. Formation of the quartz trench by the second write as defined by resist needs further understanding and optimization. The image shift, seen on the chromeless dense lines, will also need to be characterized for isolated lines and on other exposure tools where NA is increased.

ACKNOWLEDGEMENTS

The authors wish to thank Melinda Nemec and Josie Fisher of Photronics for their help with fabrication of the mask, Betty Ann Blachowicz and Marco Vieira of ARCH Chemical for their help with the wafer print and SEM work they did. We would also like to thank Chris Mack of KLA Tencor's Finle Technology for the ProMax simulation support.

REFERENCES

1) C.M. Wang, C.W. Lai, J. Huang, H.Y. Liu, SPIE Vol 4346, pg. 452 (2001)
2) C. Nelson Thomas, M.E. Kling, M.A. Thompson, R. Wang, N. Cave, C.C. Fu, SPIE Vol. 4346, pg. 464 (2001)
3) R. Chau, J. Kavalieros, B. Roberts, R. Shenker, D. Lionberger, D. Barlage, B. Doyle, R. Arghavani, A. Murthy, G. Dewey, IEDM 2000 Proceed., pg. 45
4) M. Fritze, J.M. Burns, P.W. Wyatt, D.K. Astolfi, T. Forte, D. Yost, P. Davis, A.V. Curtis, D.M. Preble, S.G. Cann, S. Denault, H.Y. Liu, J.C. Shaw, N.T. Sullivan, R. Brandom, M.E. Mastovich, SPIE Vol. 4000, pg. 388 (2000)
5) H.Y. Liu, L. Karlin, Y-T Yang, Y.C. Pati BACUS Vol 3236, pg 328 (1997);
6) H.Y. Liu, L. Karlin, Y-T Yang, Y.C. Pati, SPIE Vol. 3334, pg. 2 (1998)
7) M. Fritze, B. Tyrrell, D. Astolfi, D. Yost, P. Davis, B. Wheeler, R. Mallen, J. Jarmolowicz, S. Cann, H.Y. Liu, M. Ma, D. Chan, P. Rhyins, C. Carney, J.Ferri,A.Blachowicz, SPIE Vol 4346 pg 191 (2001)
8) R. Shenker, SPIE Vol 3679, pg 18 (1999)
9) 1999 International Technology Roadmap for Semiconductors, www.itrs.net/1999_SIA_Roadmap/Home.htm
10) H.Y. Liu, L. Karlin, Y-T Yang, Y.C. Pati, SPIE vol 3334, pg 11 (1998)
11) R. Schmidt, C. Spense, L. Capodieci, Z. Krivokapic, B. Geh, D. Flagello, SPIE vol 3334, pg 15 (1998)
12) M. Fritze, S. G. Cann, P, Wyatt, SPIE vol 3679, pg 567 (1999)